Post VSD aided test column characterization of consolidation properties of oil sands tailings

Moir D. Haug, Julian Gan & Mohammad Al-Mamun
SNC-Lavalin Inc., Saskatoon, Saskatchewan, Canada

ABSTRACT
The consolidation characteristics of oil sands tailings subjected to 60 kPa of total stress surcharge loading in a vertical strip drain (VSD) aided, 0.52-m diameter 4-m high fully instrumented test column were evaluated following three plus years of testing. Large diameter consolidation test specimens taken at different depths during the test column decommissioning were subjected to large strain consolidation (LCS) testing, using pressures up to 1000 kPa. Void ratios of samples collected near the VSD and the wall of the test column were used in combination with calculated effective stress to establish a relationship between void ratio and effective stress for the test column. This relationship showed good agreement with pre-test column LSC test results. The post-test column LSC test results also agreed well with the pre-test column LSC test at effective stress level levels above 100 kPa. Back projection of the virgin compression curves indicate a potential "base-line" for evaluating the impact of various additives on oil sands consolidation.

RÉSUMÉ
Les caractéristiques de consolidation des résidus de sables bitumineux soumis à une charge de surcharge totale de 60 kPa dans une colonne d'essai entièrement instrumentée assistée par un drain à bande verticale de 0,52 m de diamètre et de 0,52 m de diamètre ont été évaluées après plus de trois ans d'essais. Les éprouvettes de consolidation de grand diamètre prélevées à différentes profondeurs pendant le déclassement de la colonne de test ont été soumises à des essais de consolidation de grandes déformations (LCS), à des pressions allant jusqu'à 1000 kPa. Les taux de vide des échantillons prélevés près du VSD et de la paroi de la colonne de test ont été utilisés en combinaison avec la contrainte effective calculée pour établir une relation entre le taux de vide et la contrainte effective de la colonne de test. Cette relation a montré une bonne concordance avec les résultats du test LSC sur colonne pré-test. Les résultats du test LSC sur colonne post-test sont également en bon accord avec le test LSC sur colonne pré-test à des niveaux de contrainte effectifs supérieurs à 100 kPa. Les rétroprojections des courbes de compression vierges indiquent une «ligne de base» potentielle pour évaluer l'impact de divers additifs sur la consolidation des sables bitumineux.

1 INTRODUCTION

This paper presents the results of post-test column laboratory testing and analysis of oil sand tailings. It builds on the work of Gan et al, 2018, which described the results of a test column study to evaluate the performance of vertical strip drains (VSD) in enhancing the consolidation of oil sands tailings.

Znidarcic et al., 2011, reported that oil sands tailings in the field consolidate "extremely" slowly; to the point where there is a question as to whether or not consolidation theory adequately describes the settlement process at low levels of effective stress. In order to address this uncertainty, different techniques have been used to evaluate the consolidation of oil sands tailings. These have included the development of large-strain consolidation (LSC) test apparatus employing direct loading (Pollock, 1988, Suthaker, 1995, Gan et al., 2014, etc.), seepage induced consolidation (SICT) test apparatus (Estepho, 2011, Znidarcic, et al., 2011, etc.) and centrifuge testing (Sorta, 2015). A number of settlement test columns have also been constructed to investigate the consolidation of oil sand tailings (Suthaker, 1995, Stianson, et al., 2016, Haug, et al., 2018); however, adequately describing the consolidation characteristics of oil sands tailings remains challenging. And, this is especially the case at low level of effective stress where interparticle forces play a major role in consolidation (Jeeravipoolavarn, 2005.

The first objective of this paper was to compare the results of laboratory LSC testing with the results from a large diameter test column tests conducted on the same oil sands tailings. A second objective was to determine if a base-line, or back calculated virgin compression curve could be established for the oil sands tailings which would be consistent with both LSC and consolidated test column tailings. If such a base-line curve can be established, it might provide a valuable reference for evaluating the settlement potential of fine oil sands tailings at low levels of effective stress.

2 BACKGROUND

2.1 Material Characteristics

The oil sand tailings used for this study were obtained from near the surface of an oil sands tailings storage facility (TSF), and known as mature fine tailings (MFT). These slurried tailings had dewatered to a water content of 114 % under self-weight loading, freeze-thaw cycles and evaporation. A summary of the MFT characterization is presented in Table 1. The tailings had an initial average solids content, water content and liquid limit of 47.3 %, 114 %, and 47.7 % respectively. The liquidity index was 2.2, indicating the slurry nature of the material. The specific gravity of the tailings was 2.12. The bulk density of the tailings was 1.35 Mg/m^3 and the sand to fines ratio (SFR) was

0.2. The tailings had a bitumen content of 4.5 % based on total weight.

Table 1 Tailings Characteristics (from Haug et al., 2018)

Property	Value
Initial water content (%)	114.4
Initial solids content	47.3
Bulk density (Mg/m^3)	1.35
Solids specific Gravity	2.12
Mineral content (Mass solids) %	43.0
Mass water (%)	52.0
Mass bitumen (%)	4.50
Sand to fines (<0.44 mm) ratio (SFR)	0.2
Liquid Limit (%)	47.7
Plastic Limit (%)	17.7

2.2 Test Column Study

Phase I and phase II test column studies were conducted to evaluate the effectiveness of vertical strip drains (VSD's) in enhancing the consolidation of oil sand tailing. These test columns were fully instrumented. The ~6 month phase I study (Haug et al., 2018) involved self-weight consolidation. The 3.2 year phase II study involved the application of 60 kPa of surcharge loading (Gan et al., 2018). At the end of each phase the columns were dismantled and was carefully sampled throughout (decommissioning). LSC and other tests were also conducted on the tailings both before (pre) and after (post) column testing.

3 LARGE STRAIN CONSOLIDATION (LSC) AND POST-COLUMN TESTING

Figure 1 shows a photograph of one of the LSC test apparatus used in this program for both pre-column test and post-column test samples. The apparatus consists of 150 mm diameter by 150 mm high stainless steel cells with 50 mm high extension rings. Initial loading is carried out using a counter weight system to enable measurement of consolidation of soft, highly compressible tailings. Stepped direct loading is used to reach 500 kPa, with total testing time taking 3 to 5 months. At that stage the samples are "intact" and can be transferred to larger test apparatus for continued loading up to 5000 kPa; if required to establish the virgin compression curve. A constant head device was used to maintain continuous flow during the entire 3 to 6 months of the test. This photo also shows plastic film covering over the sample to minimize evaporation during testing.

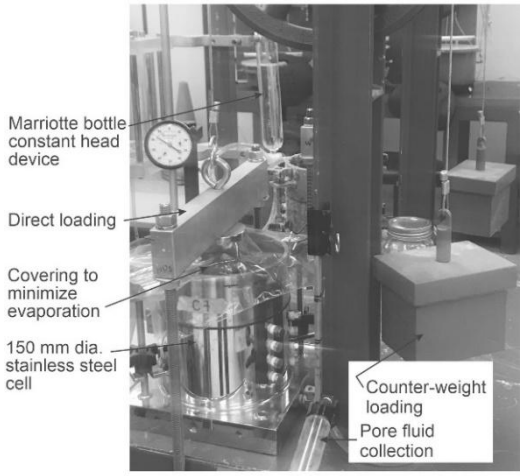

Figure 1 LSC testing of pre-test column MFT (Haug et al., 2018)

Figure 2 shows the pre-column test LSC test carried out on the tailings (Haug, et al., 2018). Both void ratio and solids content are shown as a function of applied load. The initial water content of the tailings was approximately 114 % (i.e. void ratio 2.4). At the end of the LSC test the water content was approximately 18 %. Hydraulic gradients used for hydraulic conductivity testing are low (typically less than 1); however, it does result in a small additional seepage gradient (stress). The "adjusted" data points reflects this increase in load. The overall compression index (C_c) for the adjusted relationship is 0.56; however, the change in the slope of the curve above 100 kPa (last three data points) suggests a C_c of 0.35. This agrees with the 0.34 value predicted by equation 1 (Skempton, 1944) using the liquid limit from Table 1.

$$C_c = 0.009\ (LL - 10) \qquad [1]$$

Post-column testing involved water content, density, vane shear strength, and other characterization tests. Large diameter samples were collected from the phase II test column for LSC testing. These consolidations tests specimens were loaded up to maximum values of either 500 or 1000 kPa, over a six month plus time period.

4 TEST COLUMN LAYOUT

The Phase I and Phase II test columns were fabricated from 525 mm diameter ribbed PVC pipe. The Phase I self-weight test column contained 1.738 m of tailings surrounding a central VSD. The VSD allowed the tailings to drain through a port in the base which was connected to tubing extending upwards along the column to an outflow maintained at the same elevation as the MFT inside the test column. Ten manometers were placed at roughly even spaces along the sides of the test column and three across the base. These manometers were designed to measure the drop-in pore pressure with time as the

MFT settled. The elevation of the surface of the MFT was monitored magnetically.

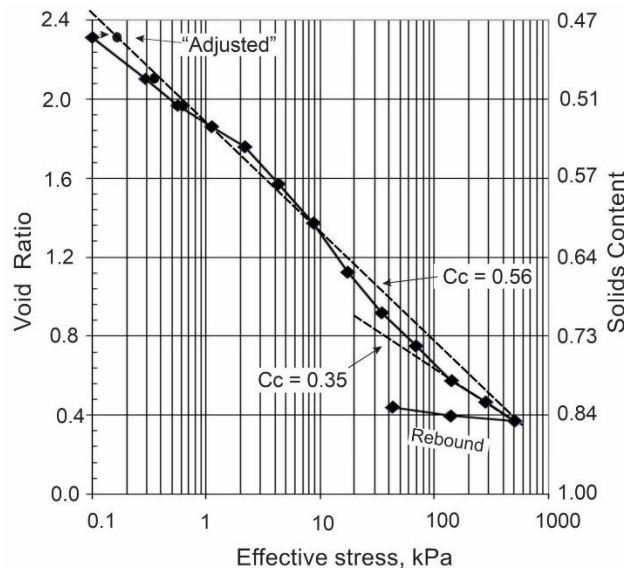

Figure 2 LSC testing of pre-test column MFT (redrawn after Gan et al, 2011).

A photograph of the Phase II test column is shown in Figure 3. This 3.4 m high test column contained a 1.537 m high central VSD surrounded by 2.7 m of slurried tailings. The slurried tailings were cover with a water cap maintained at an elevation of 3.012 m. The top of the test column was sealed to enable the application of up to 60 kPa of surcharge loading on the tailings.

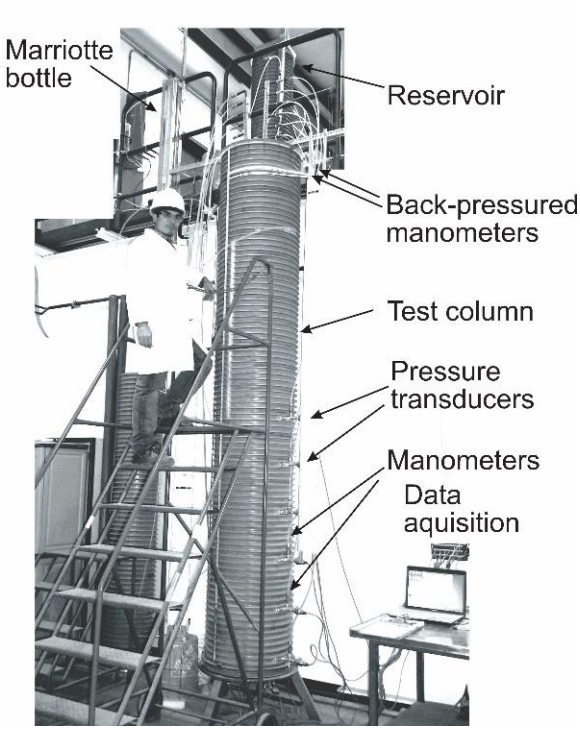

Figure 3 Photograph of phase II test column

The initial surcharge loading was 40 kPa and this was increased to 60 kPa part-way through the test. A constant head device was used to maintain the water level at elevation 3.012 m in the test column. The test column was instrumented with a series of pressure transducers and back-pressured manometers.

At the end of the column test, the column was dismantled in horizontal sections. This was done to expose the surface of the MFT and allow for sampling and in situ strength testing (vane shear). Figure 4 shows that the MFT filled test column was divided into layers from Layer 0 just above the elevation of the top of the VSD to Layer 9 at the bottom.

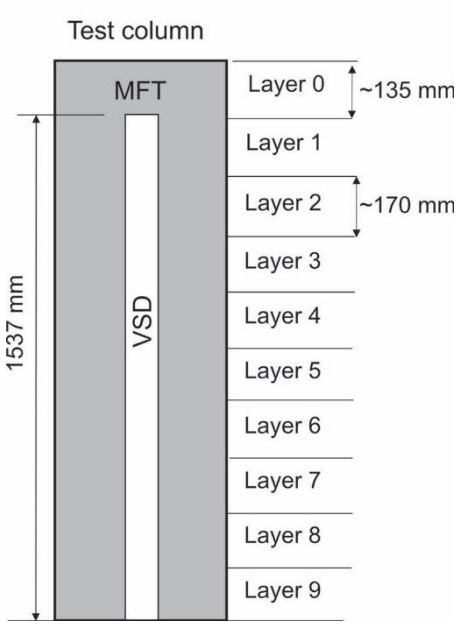

Figure 4 Phase II test column sectioning plan (Gan et al., 2018)

5 DECOMMISSIONING AND SAMPLING OF THE TEST COLUMN

Figure 5 shows the aluminum sampling grid constructed to aid in controlled sample collection with depth. The grid contains 22 locations for water content sampling. The VSD is partially visible near the center of the column. The upper portion of the VSD had shifted sideways from its location adjacent cells 13 and 14. A geophysical sampling tube is also shown adjacent the VSD. This device was intended to measure changes in water content with depth during the test; however, it was not possible to get reliable measurements due to various interference.

Water content samples were collected at all of the grid layer locations. The LSC sampling location is also shown in Figure 5.

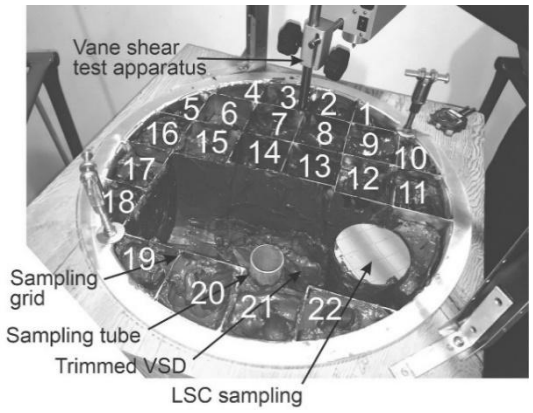

Figure 5 Post-test aluminum sampling grid

Figure 6 shows one of the LSC samples collected for post-test column consolidation (reconsolidation) testing. LSC samples were collected at layers 4, 6 and 8; and the x-y position of all sample was identical. The sample shown was collected from layer 6 and transferred to an LSC test apparatus for testing.

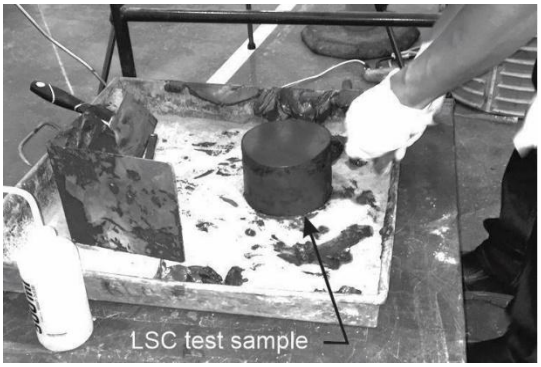

Figure 6 Collection of large diameter sample for LSC testing

Figure 7 shows the stress distributions within the test column at the end of the test. Total stress was calculated based on average bulk density of the tailings. Pore pressure were measured along the VSD and wall of the test column. The height of the discharge tube controlled the hydrostatic pressure inside the VSD, as indicated by a thick dark line on the drawing. The total stress is shown as a heavy dashed line. At the top of the MFT the total stress was 73.14 kPa, 60 kPa of which was due to the surcharge load. At the base of the VSD the total stress was 98.78 kPa. The effective stress developed is represented by the total stress line minus the pore pressure at that location.

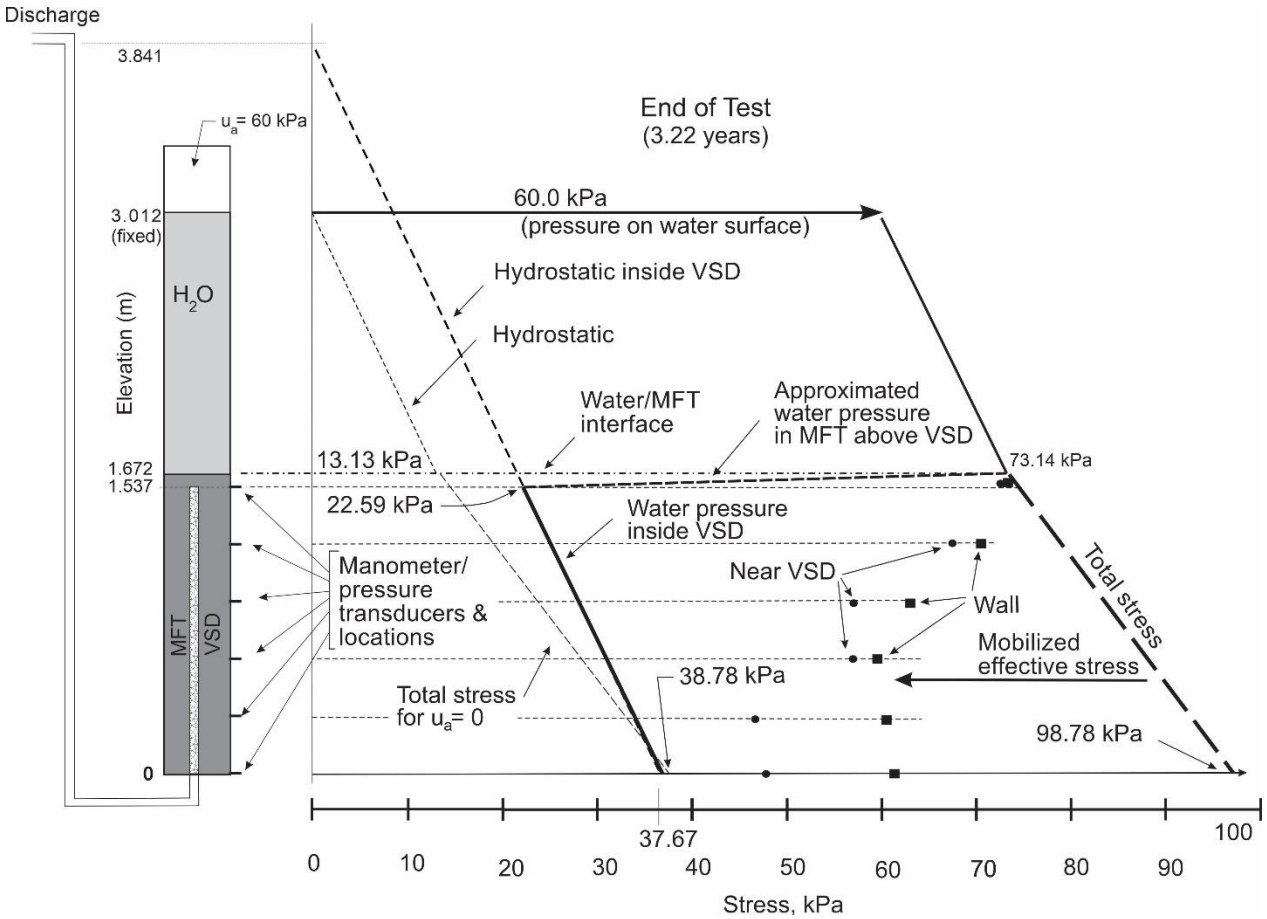

Figure 7 End of column test stress distributions (redrawn after Gan et al., 2018)

6 ANALYSIS

6.1 Test column and LSC void ratio versus water content comparisons

Figure 8 shows end-of-test calculated effective stress development within the MFT as a function of test column elevation. These plots are based on data presented in Figure 7. The relationships shown are for both the near VSD and the wall instrumentation.

The effective stress developed near the VSD increased from "0" at the surface of the MFT (elevation 1.672 m) linear with depth to a little over 50 kPa at the base of the test column. The maximum potential effective stress build up at the base of the column is 61.1 kPa based on a total stress of 98.78 kPa and hydrostatic pressure of 37.67 kPa. A "short-dashed" line linear regression analysis produced a best fit relationship having a correlation coefficient of -0.9925.

The effective stress developed at the wall of the test column is also shown on this figure. It increases from zero at the surface linearly with depth to 38.9 kPa at the base of the test column. A "long-dashed" line linear regression analysis produced a slightly weaker correlation coefficient of 0.9757.

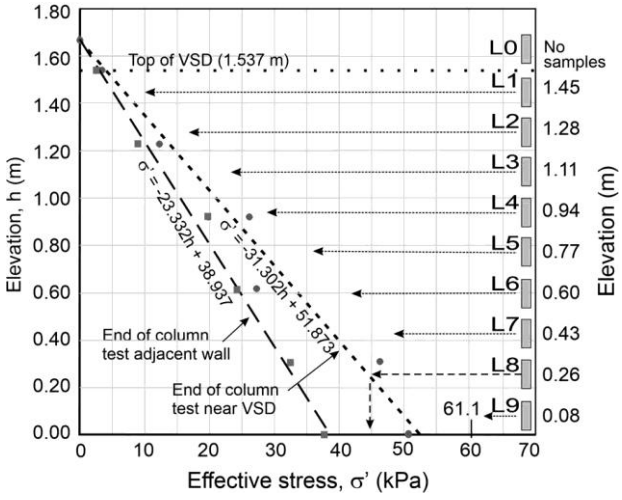

Figure 8 Effective stress development with depth for near the VSD and wall pore pressures

Figure 8 also shows the approximate elevation of water content sampling carried out as the test column was cut down in sections (L0 to L9). This portion of the figure is based on Figure 4, and is intended to illustrate the process of determining the effective stress of samples collected for water content measurements. For example, a water content sample collected near the VSD in Layer 8 (elevation 0.26 m) would have developed approximately 45 kPa of effective stress (dashed line).

Figure 9 shows the variation in water content and void ratio with depth within the test column. The void ratios were calculated from Equation 2.

$$Gw = Se \qquad [2],$$

where, G is the specific gravity (from Table 1), S is the degree of saturation (1.0) and W s the water content. The sample elevations shown are based on measurements taken during the dismantling, and differ to some extent from the "planned" sample layer depths. Cells 12-15 are located near the VSD and cells 11 and 16 near the walls of the test column. These show that the water contents initially drop sharply from the 70% plus range and gradually taper off with depth to the 40 % plus range. The water contents near the VSD are consistently lower diverging more near the top and bottom of the test column.

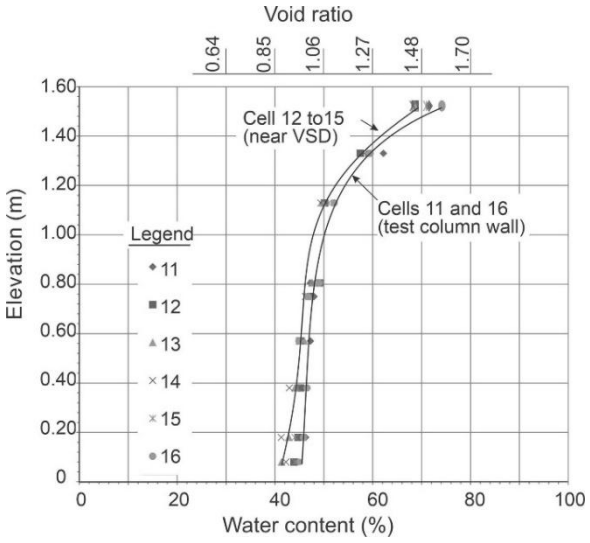

Figure 9 Variation in MFT water content and void ratio (based on known specific gravity and saturated conditions) with test column depth

MFT test column sample void ratios collected near the VSD and adjacent the wall are shown in Figure 10, as a function of effective stress (from Figure's 8 and 9). Overlaying the test column data with the pre LSC test results shows good agreement between the LSC and the test column for effective stress values in excess of 8 kPa.

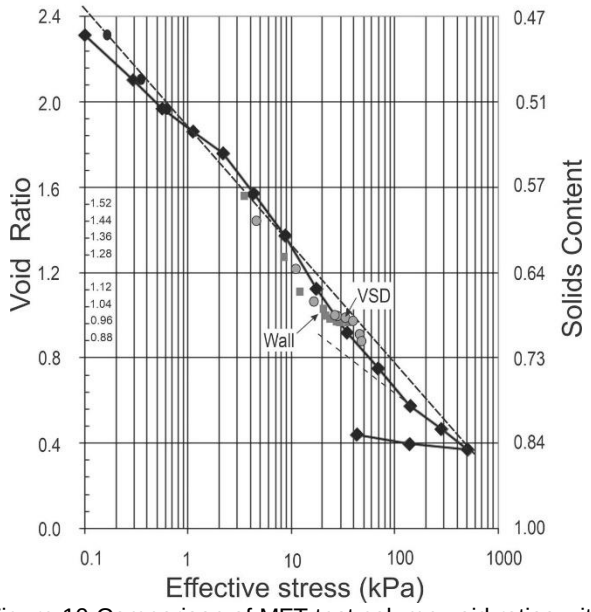

Figure 10 Comparison of MFT test column void ratios with developed effective stress to LSC test results.

6.2 Nature of the stress strain relationships

A number of tests have been conducted using different methods to measure the consolidation of oil sand tailings having low SFR's. Figure 11 shows a comparison of large strain consolidation tests conducted on similar low SFR oil sands tailings; and illustrated how initial void ratio affects consolidation characteristics. Pollock, 1988 conducted large strain consolidation test (1) on oil sand sludge having an initial void ratio of 5.8 (solids content of 30 %) and a SFR of approximately 1 and 7 % bitumen by weight. The oil sands tailings were placed into a stainless steel consolidation cell to settle/drain under self weight consolidation. Once that was completed, a loading cap installed and the step loading consolidation test initiated. These tailings consolidated quickly with load and levelled off to a constant slope near 10 kPa.

Figure 11 also shows the results of two large strain consolidation test (2a and 2b) conducted by Suthaker, 1995. The two sets of 3 % bitumen tailings had plastic and liquid limits of 23 % and 59 % respectively, and each had different solids content and void ratio. These plots were redrawn by Jeeravipoolvarn, 2005. In the first test the initial void ratio was 9.1. The tailings initially consolidated slowly with increase in effective stress, then more quickly before levelling off to a degree at near 10 kPa. The second sample had an initial void ratio of 7.3 (25 % solids content). This sample had a similar pattern and level off near 30 kPa of effective stress. Both of these samples levelled off with a void ratio 0.6 higher than the void ratio found by Pollock, 1988.

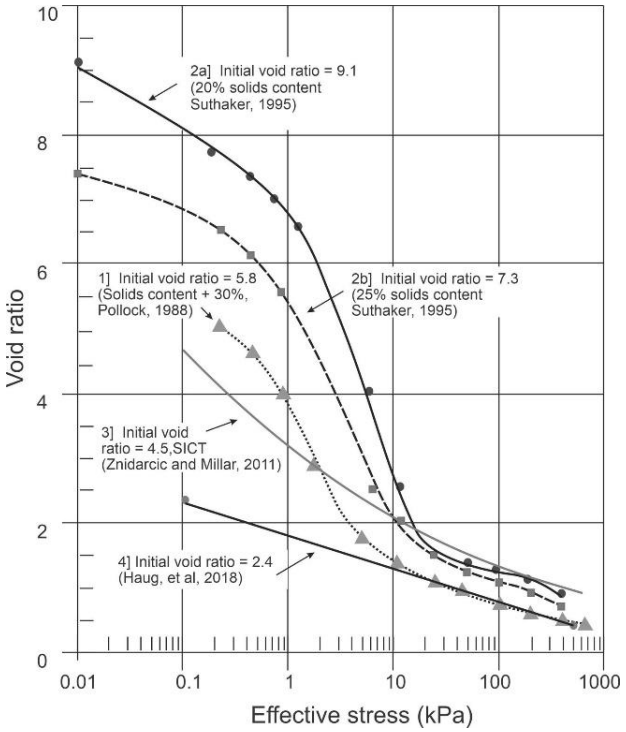

Figure 11 Comparison of large strain consolidation test results for similar oil sands materials

The fourth consolidation plot (3) shown on this figure is from Znidarcic et al., 2011. This sample was collected from the sample TSF as the tailings used in this test program. Seepage induced consolidation testing (SICT) was used in this test. The shape of this plot shows a gradual decrease in consolidation rate with the slope levelling off at a void ratio 0.8 higher than the value shown by Pollock (loc. sit.). No reverse curvature is visible.

The relationship for the fifth plot (4) was from the current study (Figure 2). The changes in scale suggest that the relationship between void ratio and effective stress is nearly linear; however, all of the other plots except for the SICT test show reverse curvature.

The concept of reverse curvature for oil sands tailing compression is counter to the opinion of Monte and Krizek's, 1976 fluid limit concept; which proposed that as the effective stress approaches zero, that the void ratio should become infinite. This would also suggest that as these materials approach "zero" effective stress, their void ratios would be the same. Pollock (loc. sit.) pointed out that numerous researchers (Salem and Krizek, 1974 and Znidaracic et al., 1986. etc.) have shown that slurry void curvatures vary from soil to soil at low levels of effective stress, and thus, the reverse curvature is not unexpected.

Figure 12 contains a plot of void ratio and solids content versus effective stress for post-test column tests (reconsolidation). These tests were conducted on samples collected during dismantling of the test column. The samples were obtained from layers 4, 6 and 8. Two of the test specimens were loaded in steps up to 500 kPa, with the sample from layer 8 loaded to 1000 kPa. The relatively "flat" nature of the consolidation curves made definition of pre-consolidation pressures challenging. Estimated pre-consolidation pressures (Pc) for layers 4, 6 and 8 were 20, 27 and 35 kPa, respectively. This compares to Figure 8 predicted values for layers 4, 6 and 8 (based on near VSD and wall estimates) of 15 to 23 kPa, 25 to 33 kPa, and 32 to 44 kPa, respectively.

The compression indexes for all three consolidation curves was approximately 0.35, and the straight line portion of the consolidation curve closely approximate the LSC test results. The C_c value was the same as that obtained for the LSC test (in the range above 100 kPa of effective stress). This suggests that the virgin compression curve for this material is well represented by the four nearly parallel lines shown in Figure 12.

6.3 Establishment of a consolidation "base-line"

Figure 13 shows an exaggerated vertical scale of void ratio and solids content versus effective stress, for the LSC test and the three consolidation tests. In this figure, the slope of the virgin compression curve developed for effective stress values in excess of 100 kPa, has been projected backwards up the slope to a value of just above a void ratio of 1.6 at 0.1 kPa of effective stress. The zone between this line and the LSC pre-test column test represents the potentially "impacted" (flocculants, dispersants and polymers) zone. In this case the back projected virgin compression curve would represent a naturally occurring normally consolidated soil; and could provide a potential base-line for evaluating the impact of dispersants and flocculants on the consolidation of the tailings. It might also provide a means of evaluating the various consolidation relationships obtained in the laboratory, such as the time dependency parameter suggested by Suthaker, 1995; aging, and others.

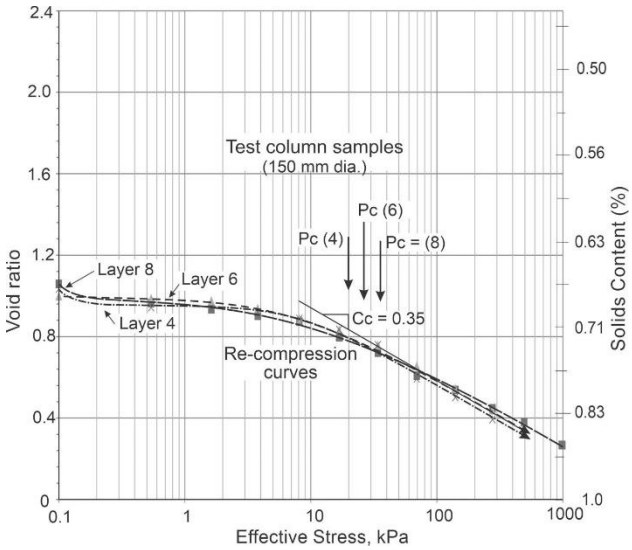

Figure 12 LSC test curves for test column samples

7 SUMMARY AND CONCLUSIONS

This test program found good agreement between post-test column consolidation tests and pre-test column long duration LSC test (Figure 13). Three large diameter MFT

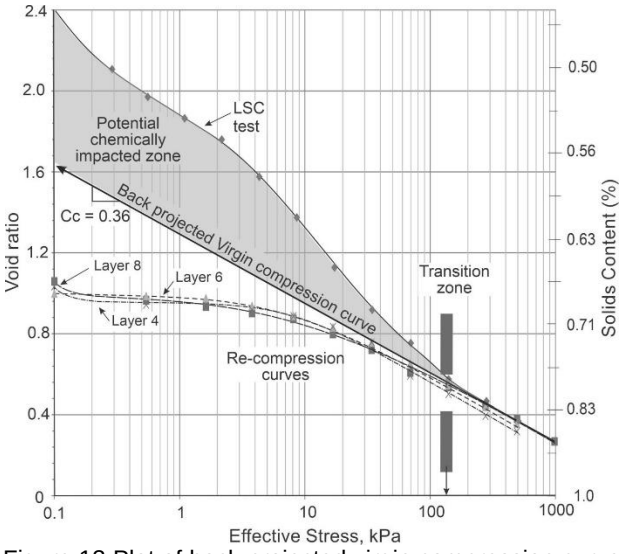

Figure 13 Plot of back projected virgin compression curve in comparison with pre-test LSC test and test column consolidation curves.

samples were collected at different column depths during dismantling. These samples were subjected to consolidation testing. The near end-of-test straight line void ratio versus effective stress plots closely matched, and their compression indexes were nearly identical. The compression indexes also agreed closely with the value predicted by Skempton's liquid limit based equation (Eq. 1), for normally consolidated clays.

Reasonably good agreement was also found between the estimated pre-consolidation pressure of the three post-test column consolidation MFT samples and the calculated maximum level of developed effective stress during the test column's 3.2 years of testing.

Good agreement was also found between the consolidated state of MFT in the test column, and that predicted by the LSC test. The void ratios of the water content samples collected throughout the test column were calculated, based on the assumption that the samples were saturated and had a consistent specific gravity. This included samples near the VSD and those near the wall of the tests column. The effective stress developed at each of the water content sample locations was determined by subtracting the interpolated pore pressure values from the calculated total stress. The calculated void ratio and developed effective stress values were plotted against the LSC test results in Figure 10, and showed good agreement.

One of the three test column consolidation test was loaded up to 1000 kPa. The straight line portion of that curve along with the plots from the two other consolidation curves agreed closely. They also agreed well with the pre-test column LSC test at loading levels above 100 kPa. This suggest that these "lines" represent the virgin compression curve for this MFT. And, if this is the case, back projection could potentially represent a "base-line" for evaluating the impact of additives on oil sands tailings consolidation. It could also be used to investigate different phenomena such as flocculation and the break-down of flocs at low levels of effective stress. In addition, it could aid in the investigation of aging, impact of freeze-thaw cycles, etc. on tailings consolidation. The precision of the back projection could also be potentially improved by increasing the LSC loading above 1000 kPa. This could provide greater confidence in the position of the virgin compression curve.

8 REFERENCES

Estepho, Mathiew, 2014. Seepage Induced Consolidation Test: Characterization of mature fine tailings. Ph.D. Thesis, Faculty of Mining Engineering, University of British Columbia.

Gan, Julian, Haug, Moir D., and Mohammad Al-Mamun. 2018. Impact of surcharge loading on VSD performance in dewatering oil sands tailings. Proceedings *Canadian Geotechnical Conference*, Edmonton, Alberta.

Haug, Moir D, Gan, Julian, and Mohammad Al-Mamun. 2018. Test column study into VSD aided self-weight consolidation of oil sands tailings. Proceedings *Canadian Geotechnical Conference*, Edmonton, Alberta.

Jeeravipoolavarn, Silawat. 2005. Compression of Oil Sands Tailings. *M.Sc. Thesis*, University of Alberta, Edmonton, Alberta.

Monte, J.L. and Krizek, R.J., 1976. One-dimensional Mathematical Model for Large-Strain Consolidation. *Geotechnique*, Vol. 26, No. 3. pp 495-510.

Pollock, G.W. 1998. Large strain consolidation of oil sands tailings sludge1. *M.Sc. Thesis*, University of Alberta, Edmonton, Alberta. P276.

Salem, A.M. and Krizek, R.J. 1973. Consolidation Characteristics of Dredging Slurries. ASCE *Journal of Waterways, Harbors and Coastal Engineering Division*, Vol. 99, WW4, pp. 439-457.

Skempton, A.W. 1944. Notes on Compressibility of Clays. *Quarterly Journal of the Geological Society of London*, Vol. 100, 119-135.

Sorta, Amarebh Refera, 2015. Centrifugal modelling of oil sand tailing consolidation. Ph.D. Thesis, Geotechnical Engineering, Department of Civil and Environmental Engineering, University of Alberta.

Stianson, Jason, Mahood, Robert, Fredlund, D. G. and Sun, Sosh, 2016. Large Strain consolidation modelling to determine representative tailings consolidation properties from two meso-scale column tests. IOSTC 2016, Lake Louise, AB, December 4-7, 2016.

Suthaker, Nagula Naguleswary. 1995. Geotechnics of Oil Sands Tailings, *Ph.D. Thesis*, University of Alberta, Edmonton, Alberta.

Znidarcic, Dobroslav, Croce, P., Pane, V. Ko, H.W., Olsen, H.W., and Schiffman, R.L. 1984. The Theory of One-Dimensional Consolidation of Saturated Clays, III, Existing Testing Procedures and Analysis. *Geotechnical Testing Journal,* Vol. 7. No. 3. pp 123-133.

Znidarcic Dobroslav, Millar, Robert, Van Zyl, Dirk, Fredlund, Murray, and Wells, Sean. 2011. Consolidation Testing of Oil Sand Fine Tailings. Proceedings *Tailings and Mine Waste 2011*, Vancouver, BC, November 6 to 9.